Editors' Suggestion | Featured in Physics

Scaling Description of Creep Flow in Amorphous Solids

Marko Popović,[1,2,3] Tom W. J. de Geus,[1] Wencheng Ji,[1] Alberto Rosso,[4] and Matthieu Wyart[1]
[1]Institute of Physics, EPFL, Lausanne, Switzerland
[2]Max Planck Institute for Physics of Complex Systems, Nöthnitzer Strasse 38, 01187 Dresden, Germany
[3]Center for Systems Biology Dresden, Pfotenhauer Strasse 108, 01307 Dresden, Germany
[4]LPTMS, CNRS, Université Paris-Sud, Université Paris-Saclay, 91405 Orsay, France

(Received 17 January 2022; revised 11 July 2022; accepted 27 September 2022; published 9 November 2022)

Amorphous solids such as coffee foam, toothpaste, or mayonnaise display a transient creep flow when a stress Σ is suddenly imposed. The associated strain rate is commonly found to decay in time as $\dot{\gamma} \sim t^{-\nu}$, followed either by arrest or by a sudden fluidization. Various empirical laws have been suggested for the creep exponent ν and fluidization time τ_f in experimental and numerical studies. Here, we postulate that plastic flow is governed by the difference between Σ and the transient yield stress $\Sigma_t(\gamma)$ that characterizes the stability of configurations visited by the system at strain γ. Assuming the analyticity of $\Sigma_t(\gamma)$ allows us to predict ν and asymptotic behaviors of τ_f in terms of properties of stationary flows. We test successfully our predictions using elastoplastic models and published experimental results.

DOI: 10.1103/PhysRevLett.129.208001

Amorphous materials including atomic glasses, colloidal suspensions, dense emulsions, or foams are important in industry and engineering [1,2]. From a fundamental viewpoint, their properties are mesmerizing: (i) under quasistatic loading they can display an avalanche-type response [3] near their yield stress Σ_c. (ii) For $\Sigma > \Sigma_c$, they can present a singular flow curve, corresponding to the so-called Herschel-Bulkley law [4] where the strain rate follows $\dot{\gamma} \approx c(\Sigma - \Sigma_c)^\beta$ with c a material-specific constant and $\beta > 1$, see, e.g., [5]. We restrict ourselves to materials with such flow curves. (iii) Depending on the system preparation the transient response to an applied strain can be smooth, or discontinuous if a narrow shear band appears [6–8]. Here, we focus on (iv) creep flows, another transient phenomenon observed when a constant stress Σ is imposed at time $t = 0$ on an initial state at zero applied stress. Transiently, a flow rate $\dot{\gamma} \sim t^{-\nu}$ is observed. At low Σ, flow eventually arrests. However, at sufficiently high Σ, $\dot{\gamma}(t)$ can be nonmonotonic: a sudden fluidization may occur at some time τ_f. Commonly, the creep flow exponent ν is measured preceding the fluidization and reported in the range $0.34 - 1.2$ in experiments [9–14] and particle simulations [15–17]. By contrast, the creep flow arrest is much less studied [12], and τ_f is often reported using phenomenological fitting functions, including (a) a power law $\tau_f \sim (\Sigma - \Sigma_0)^{-b}$ (with both b and Σ_0 fitting parameters) in experiments on carbopol microgel [11], protein gels [14], and colloidal glasses [12]; and particle simulations [15]. (b) An exponential $\ln \tau_f \sim -\Sigma$ in experiments on carbon black gels [13,18] and silica gels [19].

From a computational viewpoint, studies of creep flow in athermal elastoplastic models [20] report (a) $\tau_f \sim (\Sigma - \Sigma_0)^{-b}$ with a preparation-dependent exponent $b \simeq 1.7 - 2.2$ in a two-dimensional model [21] and $b \simeq 1.3 - 2.2$ in a mean-field model [22]. At finite temperature, both models are consistent with (b) $\ln \tau_f \sim -\Sigma$ [23]. The creep exponent ν was observed to be unity [24] or to be preparation dependent [23]. Theoretical approaches supporting particular fitting choices are mostly lacking. A notable exception is the continuum model of shear banding [25] that proposes $b = 9\beta/4$.

Here, we introduce a theoretical framework that predicts the exponent ν, the asymptotic properties of τ_f, and their dependence on temperature. We focus on long time scales and assume that flow is then essentially plastic, thus neglecting the elastic contribution to the strain. We expect this assumption to hold in the materials we consider here, coined "simple yield stress fluids" [26] such as foams, emulsions, or repulsive colloidal glasses. It does not hold in materials with a very slow linear viscoelastic response that can contribute to creep [14,27,28]. We also exclude loosely connected colloidal gels, which can display nonmonotonic flow curves and sudden transition between distinct structures [29,30]. Our central hypotheses are that the plastic flow is governed by $\Sigma - \Sigma_t(\gamma)$, where $\Sigma_t(\gamma)$ is a smooth function of plastic strain γ that characterizes the stability of configurations visited by the system at a strain γ. These assumptions lead to a comprehensive description of creep flows in terms of the Herschel-Bulkley exponent β, as is summarized in Table I for athermal and Table II for thermal

TABLE I. Main results for athermal creep flow, illustrated in Fig. 1(a). The corresponding creep flow scenarios are illustrated in Fig. 1(b), and corresponding numerical tests are shown in Fig. 2.

$\Sigma < \Sigma_M$	$\nu = \beta/(\beta-1)$
$\Sigma = \Sigma_M$	$\nu = 2\beta/(2\beta-1)$
$\Sigma > \Sigma_M$	$\tau_f \sim (\Sigma - \Sigma_M)^{(1/2)-\beta}$

systems. We confirm our predictions in two-dimensional and mean field elastoplastic models. We find that our athermal predictions are also in good agreement with experiments on carbopol microgel and colloidal glasses, while our thermal predictions are consistent with experiments on kaolin suspensions and ketchup.

Theory.—The transient response of amorphous materials strongly depends on preparation. For example, the quasistatic stress vs plastic strain curve can increase monotonically or overshoot [1,6,31] as the stability of the system preparation increases. During quasistatic loading the system is at the stress which the material can withhold without flowing at plastic strain γ. Here, we define the transient yield stress $\Sigma_t(\gamma;\Sigma,T)$ that characterizes the stability of the material for nonquasistatic loading. At zero temperature T, its definition is

$$\dot{\gamma} \equiv c[\Sigma - \Sigma_t(\gamma;\Sigma,T=0)]^{\beta}, \tag{1}$$

To lighten notations, when possible we omit the dependence of Σ_t on Σ and T and simply write it $\Sigma_t(\gamma)$. From Eq. (1), it follows that the flow arrests at the finite strain γ_a for which $\Sigma_t(\gamma_a) = \Sigma$, while in the steady state $\Sigma_t(\gamma \to \infty) = \Sigma_c$. Note that $\Sigma_t(\gamma)$ so defined can be measured by observing the creep flow dynamics and inverting Eq. (1), as performed below. Our central result is that simply assuming that $\Sigma_t(\gamma)$ is a smooth function is sufficient to determine the creep flow exponent ν and the fluidization time τ_f, see Fig. 1(b). $\Sigma_t(\gamma)$ in general depends on the preparation of the system, similar to the quasistatic stress vs strain curve. Here, we focus on the creep flow in systems where $\Sigma_t(\gamma)$ overshoots to a maximal value Σ_M before reaching its steady state value Σ_c, as illustrated in Fig. 1(a). The case where $\Sigma_t(\gamma)$ does not overshoot, and instead grows monotonically can be treated with the same

TABLE II. Main results for thermal creep flow. The corresponding numerical tests are shown in Fig. 3.

Athermal to thermal transition width	$\delta\gamma \sim T^{1/\alpha}$
Athermal to thermal transition time	$\tau_a \sim T^{(1-\beta)/\alpha}$
Thermal creep flow	$\nu = 1$
Fluidization time	$\tau_f \sim [T/(\Sigma_M - \Sigma)^{\alpha-1}]^{1/2-\beta} e^{c_T[(\Sigma_M-\Sigma)^{\alpha}/T]}$

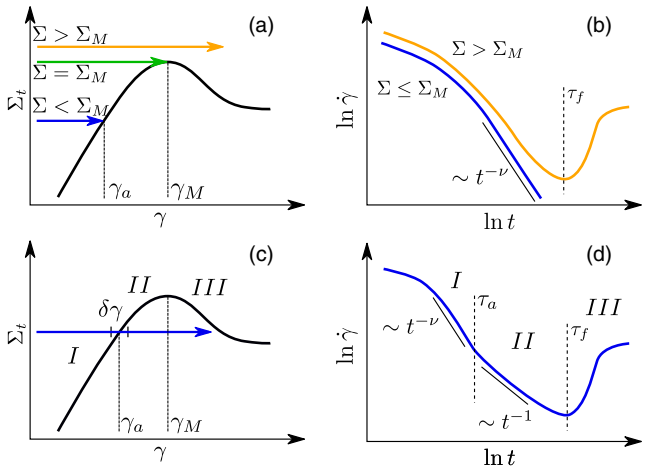

FIG. 1. Left: sketch of $\Sigma_t(\gamma;\Sigma,T)$ for (a) $T=0$ and (c) $T>0$. Arrows indicate different applied stresses Σ that lead to creep flow scenarios discussed in the text. Right: the corresponding sketch of the creep flow, respectively in (b) and (d). $\gamma_a(\Sigma)$ is defined by $\Sigma = \Sigma_t(\gamma_a,\Sigma,T)$ and $\gamma_M = \gamma_a(\Sigma_M)$.

arguments. As shown in Supplemental Material (SM) [32], the strain rate monotonically decreases to the steady state value.

At low imposed stresses $\Sigma < \Sigma_M$, the flow arrests at a finite γ_a [see Fig. 1(a)] where $\Sigma_t(\gamma_a) = \Sigma$. By expanding $\Sigma_t \simeq \Sigma_t(\gamma_a) + \partial_\gamma \Sigma_t(\gamma_a)(\gamma - \gamma_a)$ and using Eq. (1), one obtains $\dot{\gamma} \sim (\gamma_a - \gamma)^{\beta}$ implying $\dot{\gamma} \sim t^{-\beta/(\beta-1)}$. Instead, for $\Sigma = \Sigma_M = \max_\gamma \Sigma_t(\gamma) = \Sigma_t(\gamma_M)$, a second order expansion implies that $\Sigma_t(\gamma) \approx \Sigma_M + \partial_\gamma^2 \Sigma_t(\gamma_M)(\gamma - \gamma_M)^2/2$. Using again Eq. (1) one gets $\dot{\gamma} \sim (\gamma_M - \gamma)^{2\beta}$ and therefore $\dot{\gamma} \sim t^{-2\beta/(2\beta-1)}$. Finally, for $\Sigma > \Sigma_M$ the flow transiently slows down, reaching its minimum at γ_M. In the vicinity of γ_M, one has $\dot{\gamma} \sim [\Sigma - \Sigma_M + \partial_\gamma^2 \Sigma_t(\gamma_M)(\gamma_M - \gamma)^2/2]^{\beta}$. The fluidization time τ_f is the time at which γ_M is reached. It is dominated by the time spent approaching γ_M in an interval of strain of order $\Delta\gamma \sim (\Sigma - \Sigma_M)^{1/2}$, at a pace $\dot{\gamma} \sim (\Sigma - \Sigma_M)^{\beta}$, leading to a time $\tau_f \sim \Delta\gamma/\dot{\gamma} \sim (\Sigma - \Sigma_M)^{1/2-\beta}$. We summarize the athermal creep flow results in Table I.

For a small finite temperature T [37], $\Sigma_t(\gamma;\Sigma,T)$ can now be defined from the finite temperature stationary flow curves. Our qualitative results are robust to details of the functional form chosen for these curves. Quantitatively, theoretical arguments and elastoplastic models [38–41] support that the steady state flow follows a scaling relation: $\dot{\gamma} = T^{\psi} f[(\Sigma - \Sigma_c)/T^{1/\alpha}]$. Here, $\psi = \beta/\alpha$, where the parameter α describes the microscopic potential [42].

The scaling function f must be such that $\dot{\gamma}$ converges to $\dot{\gamma} \sim (\Sigma - \Sigma_c)^{\beta}$ (the Herschel-Bulkley law) in the limit $T \to 0$, i.e., $f(x) \sim x^{\beta}$ for $x \to \infty$. For negative arguments, f describes thermal activation so that $f(x) \sim \exp(-C_0 x^{\alpha})$ for $x \to -\infty$, where $C_0 > 0$.

We thus define the transient yield stress at finite T as

$$\dot{\gamma} \equiv T^{\psi} f\left(\frac{\Sigma - \Sigma_t(\gamma; \Sigma, T)}{T^{1/\alpha}}\right). \tag{2}$$

Here, we discuss systems where $\Sigma_t(\gamma)$ overshoots, as illustrated in Figs. 1(c) and 1(d), see SM [32] for the monotonic case. Initially at small strains thermal fluctuations are negligible and the creep flow exponent follows the athermal prediction $\dot{\gamma} \sim t^{-\beta/(\beta-1)}$. This regime is valid until a plastic strain γ_a for which $\Sigma \simeq \Sigma_t(\gamma_a)$, where Eq. (2) implies that the flow rate follows $\dot{\gamma} \sim T^{\psi}$. Comparing these two expressions, the crossover time where thermal activation starts to play a role follows $\tau_a \sim T^{(1-\beta)/\alpha}$. This crossover occurs on a strain increment $\delta\gamma$ [see Fig. 1(c)], which corresponds to the argument of f in Eq. (2) becoming negative and $\mathcal{O}(1)$. Expanding this argument using $\Sigma - \Sigma_t(\gamma) \sim \gamma_a - \gamma$ leads to $\delta\gamma \sim T^{1/\alpha}$. Beyond the crossover $\gamma - \gamma_a \gg \delta\gamma$, flow is dominated by thermal activation. This corresponds to the exponential behavior of $f(x)$ for large negative arguments. It is then straightforward (see SM [32]) to obtain from Eq. (2) and the linearization $\Sigma - \Sigma_t(\gamma) \sim \gamma_a - \gamma$ that the strain grows logarithmically in time, implying that $\dot{\gamma} \sim t^{-1}$ at long times. Finally, for $\gamma > \gamma_M$ the flow rate rises and fluidization occurs. In contrast to athermal systems, fluidization also occurs for $\Sigma < \Sigma_M$. We can estimate the fluidization time in the limit of small temperatures, as the time spent in the vicinity of γ_M. For $\Sigma < \Sigma_M$, expanding $\Sigma_t(\gamma)$ around γ_M in Eq. (2) and using the scaling function form we derived previously [41], we find $\tau_f \sim [T/(\Sigma_M - \Sigma)^{\alpha-1}]^{1/2-\beta} \exp[C_0(\Sigma_M - \Sigma)^{\alpha}/T]$. For $\Sigma > \Sigma_M$ the flow is predominantly athermal, except for $(\Sigma - \Sigma_M)^{\alpha} \leq T$ where $\dot{\gamma} \sim T^{\psi}$ for strains near γ_M on an interval that scales as $\Delta\gamma = \gamma_M - \gamma \sim T^{1/(2\alpha)}$, leading to a fluidization time $\tau_f \sim \Delta\gamma/\dot{\gamma} \sim T^{(1/2-\beta)/\alpha}$.

Numerical simulations.—To test the proposed creep exponents we simulate creep flow using a two-dimensional elastoplastic model [41] (see SM [32]), whereby we benefit from previously measured exponent $\beta = 1.52$ [5] and scaling function f [41].

To estimate the athermal transient yield stress function $\Sigma_t(\gamma; \Sigma, T = 0)$, we measure $\dot{\gamma}(t)$ at a tiny temperature $T = 0.002$ and then numerically invert Eq. (2) using the previously measured f [41], as shown in Fig. 2(a). We use a tiny but finite temperature to probe Σ_t beyond the strain γ_a at which athermal creep would arrest. We find that Σ_t changes with Σ, but this dependence is weak. More importantly, our observations are consistent with our smoothness assumption. For comparison, we show the quasistatic stress vs plastic strain curve in the same system, which is clearly different from $\Sigma_t(\gamma)$.

We simulate the athermal creep flow at stresses $\Sigma \leq \Sigma_M$, see Fig. 2(b). The measured creep flow dynamics is consistent with predictions summarized in Table I. To further test our predictions, we use a mean-field version of elastoplastic model [43], which corresponds to a version of the Hébraud-Lequeux model [44] where $\beta = 2$. We again find that creep flow dynamics is consistent with our predictions, see Fig. 2(c).

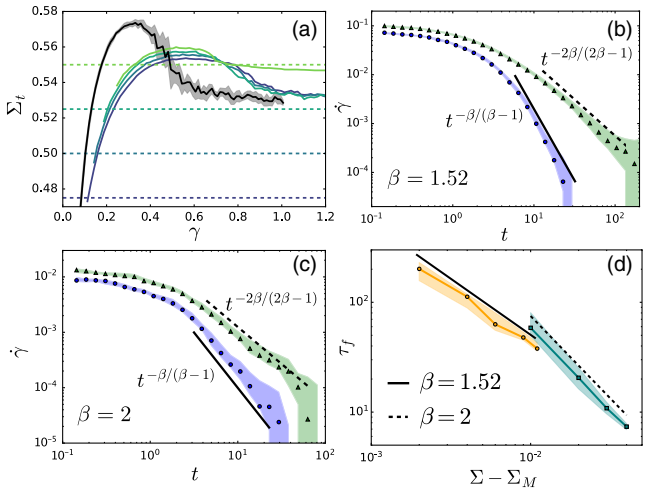

FIG. 2. Creep flow in athermal elastoplastic models. (a) Transient yield stress curves $\Sigma_t(\gamma)$ at stresses indicated by the dashed lines, at $T = 0.002$. For reference, the quasistatic stress vs plastic strain curve is shown in black. (b),(c) Median values of creep flow at two imposed stresses: blue circles ($\Sigma < \Sigma_M$), green triangles ($\Sigma = \Sigma_M$). Black lines indicate the corresponding predicted power laws, see Table I. (d) Fluidization times in $2d$ (yellow circles) and mean field (cyan squares). In all plots shaded regions correspond to the 25th–75th percentile range.

Finally, for imposed stresses $\Sigma > \Sigma_M$ we measure the fluidization times τ_f as a function of the imposed stress Σ in both models, as shown in Fig. 2(d). Although the range of data is less than a decade, the changes in the asymptotic behavior of τ_f are consistent with our predictions, for both values of β.

We next turn to thermal systems. We first study the transition from the athermal to the thermal creep regime, sketched in Figs. 1(c) and 1(d). In Fig. 3(a) we show creep curves for $\alpha = 3/2$ at $\Sigma = 0.45$ in a system with an overshoot in $\Sigma_t(\gamma)$. As the temperature is decreased toward $T = 0$, the transition between the athermal regime ($\dot{\gamma} \sim t^{-\beta/(\beta-1)}$) and thermal creep ($\dot{\gamma} \sim t^{-1}$) is indeed observed, and occurs at later times following $T^{(1-\beta)/\alpha}$, as confirmed in Fig. 3(b).

Finally, we measure fluidization times of thermal creep flow at different temperatures and imposed stresses both for $\alpha = 1$ [Fig. 3(c)] and $\alpha = 3/2$ [Fig. 3(d)]. Following [10], we define the fluidization time as the time corresponding to the minimum of the flow rate. We find an excellent collapse of the data, confirming our prediction $\tau_f \sim [T/(\Sigma_M - \Sigma)^{\alpha-1}]^{1/2-\beta} \exp\{[C_0(\Sigma_M - \Sigma)^{\alpha}/T]\}$.

Note that our theory predicts asymptotic fluidization and creep exponents in the limit of vanishing flow. Therefore,

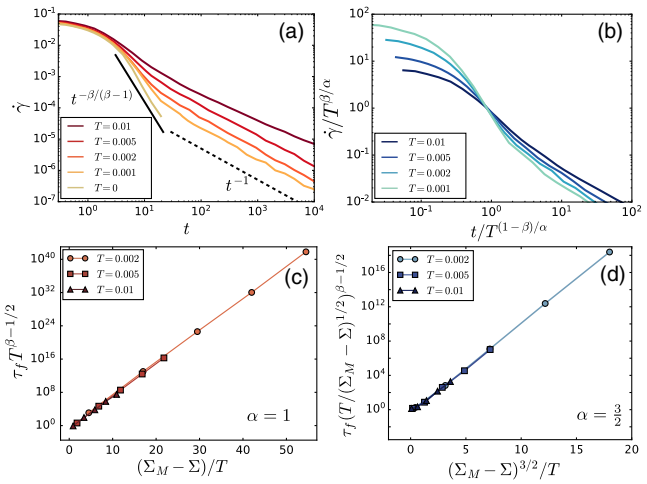

FIG. 3. Creep flow in thermal $2d$ elastoplastic model. (a) Athermal and thermal creep regimes follow the predicted flow rate exponents. (b) Rescaling flow rate and time collapses the crossing point of all curves, confirming the existence of a crossover time scale $\tau_a \sim T^{(1-\beta)/\alpha}$. (c) and (d) Fluidization times τ_f measured with $\alpha = 1$ (c) and $\alpha = 3/2$ (d) at different temperatures are consistent with our prediction.

the effective values extracted from the whole range of measured fluidization times will in general differ from our measurements. This could account for the differences to the preparation dependent effective exponents reported in the extensive numerical simulations of athermal creep in elastoplastic models [21].

Experimental tests.—We compare our results the experimental data from carbopol microgel creep experiments [11], reproduced in Fig. 4(a). At imposed stress values just below the fluidization stress, the creep exponent is consistent with our prediction $\nu = 2\beta/(2\beta-1)$, where we use $1/\beta = 0.53$ measured by [11]. We then extract the fluidization times from the minima of the flow curves both in this experiment and in the colloidal glass experiment of [12]. As shown in Fig. 4(b), it is consistent with our athermal prediction [45] $\tau_f \sim (\Sigma - \Sigma_M)^{1/2-\beta}$, as indicated

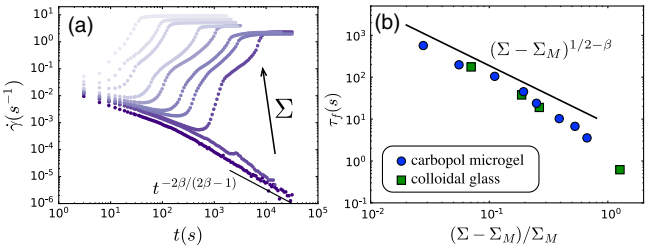

FIG. 4. (a) Creep flow of carbopol microgel [11] at $\Sigma[\mathrm{Pa}] = 35$, 36, 37, 38, 40, 43, 45, 50, 55, 60 (from bottom to top). The arresting curves are consistent with our prediction (black line). (b) Fluidization times (see main text for measurement) of carbopol microgel [11] (blue circles) and colloidal glass [12] (green squares) together with our prediction.

by the black line, where the value of Σ_M is estimated as the highest reported stress value for which no fluidization is observed, and we use $\beta = 1.89$ from [11].

Note that another definition of fluidization time τ_f^*, corresponding to the inflection point of the creep curve, was used in [11,13,18]. τ_f^* is associated with the emergence of shear banding [11,25]. Our theory for fluidization, which assumes a homogeneous flow and does not capture shear banding, may thus apply as long $\tau_f \leq \tau_f^*$. This inequality is fulfilled in the cited examples, and also in theoretical treatment supporting that the flow remains homogeneous before τ_f [46].

Concerning thermally activated creep flow, we predict an exponential dependence of τ_f on Σ, which was indeed reported in carbon black gels [13,18], and in numerical simulations of thermally activated flow in elastoplastic models [23]. Likewise, our prediction for the thermal creep flow regime $\dot{\gamma} \sim t^{-1}$ is found in numerical simulations of thermally activated flow [24]. This behavior is also found in kaolin suspensions [47] and ketchup [10]. However, the validity of our approach to these materials is less clear, as their flow curves need not follow a Herschel-Bulkley law as we assume. They can be instead thixotropic materials with nonmonotonic flow curves [48], known to shear band in stationary flows.

Discussion.—We have provided a theoretical framework in which creep flows are controlled by the stress Σ_t at which configurations visited at time t would stop flowing. Our treatment is similar in spirit to the Landau theory of a phase transition: assuming the analyticity of Σ_t enables one to express the asymptotic behaviors of creep flows in terms of the better understood stationary flows. Our analysis predicts a rich set of regimes, which is consistent with observations in elastoplastic models and in experiments.

Usual mean-field approaches, both for the yielding transition in amorphous solids [44,49] and for the depinning transition [50], consider the dynamics of the distribution $P(x)$, where x is a local variable indicating how much additional shear stress is required to have a plastic event. In such models, the rate of plastic activity following some initial condition was computed at $\Sigma = 0$ and $T = 0$ [51,52]. These results are consistent with our prediction for ν, supporting that our assumption of analyticity is equivalent to mean-field approaches as is the case in Landau theory.

Our assumption should thus break down when spatial correlations are large, which occurs, in particular, if avalanches are compact objects. It is the case for short-range depinning phenomena if the spatial dimension satisfies $d < 4$; in that case an alternative real space scaling approach summarized in SM [32] is needed. By contrast, we expect our analysis to hold if $d \geq 4$, or in amorphous solids since in that case avalanches are not compact: the density of plastic events within them vanishes as the avalanche linear extension grows [5,20].

T. G. acknowledges support from The Netherlands Organisation for Scientific Research (NWO) by a NWO Rubicon Grant No. 680-50-1520 and from the Swiss National Science Foundation (SNSF) by the SNSF Ambizione Grant No. PZ00P2_185843. The project was supported by the Simons Foundation Grant (No. 454953 Matthieu Wyart) and from the SNSF under Grant No. 200021-165509.

[1] B. Andreotti, Y. Forterre, and O. Pouliquen, *Granular Media: Between Fluid and Solid* (Cambridge University Press, Cambridge, England, 2013).
[2] D. Bonn, M. M. Denn, L. Berthier, T. Divoux, and S. Manneville, Rev. Mod. Phys. **89**, 035005 (2017).
[3] C. E. Maloney and A. Lemaitre, Phys. Rev. E **74**, 016118 (2006).
[4] W. H. Herschel and R. Bulkley, Kolloid Z. **39**, 291 (1926).
[5] J. Lin, E. Lerner, A. Rosso, and M. Wyart, Proc. Natl. Acad. Sci. U.S.A. **111**, 14382 (2014).
[6] M. Ozawa, L. Berthier, G. Biroli, A. Rosso, and G. Tarjus, Proc. Natl. Acad. Sci. U.S.A. **115**, 6656 (2018).
[7] M. Popović, T. W. J. de Geus, and M. Wyart, Phys. Rev. E **98**, 040901(R) (2018).
[8] S. M. Fielding, arXiv:2103.06782.
[9] T. Bauer, J. Oberdisse, and L. Ramos, Phys. Rev. Lett. **97**, 258303 (2006).
[10] F. Caton and C. Baravian, Rheol. Acta **47**, 601 (2008).
[11] T. Divoux, C. Barentin, and S. Manneville, Soft Matter **7**, 8409 (2011).
[12] M. Siebenbürger, M. Ballauff, and T. Voigtmann, Phys. Rev. Lett. **108**, 255701 (2012).
[13] V. Grenard, T. Divoux, N. Taberlet, and S. Manneville, Soft Matter **10**, 1555 (2014).
[14] M. Leocmach, C. Perge, T. Divoux, and S. Manneville, Phys. Rev. Lett. **113**, 038303 (2014).
[15] P. Chaudhuri and J. Horbach, Phys. Rev. E **88**, 040301(R) (2013).
[16] B. J. Landrum, W. B. Russel, and R. N. Zia, J. Rheol. **60**, 783 (2016).
[17] R. Cabriolu, J. Horbach, P. Chaudhuri, and K. Martens, Soft Matter **15**, 415 (2019).
[18] T. Gibaud, D. Frelat, and S. Manneville, Soft Matter **6**, 3482 (2010).
[19] J. Sprakel, S. B. Lindström, T. E. Kodger, and D. A. Weitz, Phys. Rev. Lett. **106**, 248303 (2011).
[20] A. Nicolas, E. E. Ferrero, K. Martens, and J.-L. Barrat, Rev. Mod. Phys. **90**, 045006 (2018).
[21] C. Liu, E. E. Ferrero, K. Martens, and J.-L. Barrat, Soft Matter **14**, 8306 (2018).
[22] C. Liu, K. Martens, and J.-L. Barrat, Phys. Rev. Lett. **120**, 028004 (2018).
[23] S. Merabia and F. Detcheverry, Europhys. Lett. **116**, 46003 (2016).
[24] D. Bouttes and D. Vandembroucq, AIP Conf. Proc. **1518**, 481 (2013).
[25] R. Benzi, T. Divoux, C. Barentin, S. Manneville, M. Sbragaglia, and F. Toschi, Phys. Rev. Lett. **123**, 248001 (2019).
[26] G. Ovarlez, L. Tocquer, F. Bertrand, and P. Coussot, Soft Matter **9**, 5540 (2013).
[27] S. Aime, L. Ramos, and L. Cipelletti, Proc. Natl. Acad. Sci. U.S.A. **115**, 3587 (2018).
[28] S. Aime, L. Cipelletti, and L. Ramos, J. Rheol. **62**, 1429 (2018).
[29] S. B. Lindström, T. E. Kodger, J. Sprakel, and D. A. Weitz, Soft Matter **8**, 3657 (2012).
[30] J. H. Cho and I. Bischofberger, Soft Matter (2022).
[31] J. Antonaglia, X. Xie, G. Schwarz, M. Wraith, J. Qiao, Y. Zhang, P. Liaw, J. Uhl, and K. Dahmen, Sci. Rep. **4**, 4382 (2015).
[32] See Supplemental Material at http://link.aps.org/supplemental/10.1103/PhysRevLett.129.208001, which includes Refs. [33–36].
[33] J. Lin, T. Gueudré, A. Rosso, and M. Wyart, Phys. Rev. Lett. **115**, 168001 (2015).
[34] A. B. Kolton, A. Rosso, E. V. Albano, and T. Giamarchi, Phys. Rev. B **74**, 140201(R) (2006).
[35] E. E. Ferrero, S. Bustingorry, and A. B. Kolton, Phys. Rev. E **87**, 032122 (2013).
[36] G. Picard, A. Ajdari, F. Lequeux, and L. Bocquet, Phys. Rev. E **71**, 010501(R) (2005).
[37] Corresponding to $T \ll T_g$, where T_g is the glass transition temperature.
[38] J. Chattoraj, C. Caroli, and A. Lemaitre, Phys. Rev. Lett. **105**, 266001 (2010).
[39] V. H. Purrello, J. L. Iguain, A. B. Kolton, and E. A. Jagla, Phys. Rev. E **96**, 022112 (2017).
[40] E. E. Ferrero, A. B. Kolton, and E. A. Jagla, Phys. Rev. Mater. **5**, 115602 (2021).
[41] M. Popović, T. W. J. de Geus, W. Ji, and M. Wyart, Phys. Rev. E **104**, 025010 (2021).
[42] The exponent α characterizes how the energy barrier ΔE associated to a plastic event depends on the additional stress $\Delta\Sigma$ needed to trigger it, as $\Delta E \sim \Delta\Sigma^{\alpha}$. For smooth interaction potentials between particles, plastic rearrangements correspond to saddle node bifurcations and $\alpha = 3/2$. For a potential with cusps $\alpha = 2$, as occurs, for example, in foams or in the vertex model of tissues [43].
[43] M. Popović, V. Druelle, N. A. Dye, F. Jülicher, and M. Wyart, New J. Phys. **23**, 033004 (2021).
[44] P. Hébraud and F. Lequeux, Phys. Rev. Lett. **81**, 2934 (1998).
[45] The steady state flow is reported to follow the Herschel-Bulkley law and therefore we expect the athermal regime to be relevant.
[46] R. L. Moorcroft and S. M. Fielding, Phys. Rev. Lett. **110**, 086001 (2013).
[47] P. Uhlherr, J. Guo, C. Tiu, X.-M. Zhang, J.-Q. Zhou, and T.-N. Fang, J. Non-Newtonian Fluid Mech. **125**, 101 (2005).
[48] G. Ovarlez, S. Rodts, X. Chateau, and P. Coussot, Rheol. Acta **48**, 831 (2009).
[49] J. Lin and M. Wyart, Phys. Rev. X **6**, 011005 (2016).
[50] D. S. Fisher, Phys. Rep. **301**, 113 (1998).
[51] P. Sollich, F. Lequeux, P. Hébraud, and M. E. Cates, Phys. Rev. Lett. **78**, 2020 (1997).
[52] J. T. Parley, S. M. Fielding, and P. Sollich, Phys. Fluids **32**, 127104 (2020).